ADVANCES IN ATMOSPHERIC SCIENCES, 2025

• Original Paper •

Record High Temperatures in the Ocean in 2024

Lijing CHENG*[1], John ABRAHAM[2], Kevin E. TRENBERTH[3,4], James REAGAN[5], Huai-Min ZHANG[6], Andrea STORTO[7], Karina VON SCHUCKMANN[8], Yuying PAN[1], Yujing ZHU[1], Michael E. MANN[9], Jiang ZHU[1,2], Fan WANG[10], Fujiang YU[11], Ricardo LOCARNINI[5], John FASULLO[3], Boyin HUANG[6], Garrett GRAHAM[12], Xungang YIN[6], Viktor GOURETSKI[1], Fei ZHENG[1], Yuanlong LI[10], Bin ZHANG[10,13], Liying WAN[11], Xingrong CHEN[11], Dakui WANG[11], Licheng FENG[11], Xiangzhou SONG[14], Yulong LIU[15], Franco RESEGHETTI[16], Simona SIMONCELLI[16], Gengxin CHEN[17], Rongwang ZHANG[17], Alexey MISHONOV[5,18], Zhetao TAN[1], Wangxu WEI[1], Huifeng YUAN[19], Guancheng LI[20], Qiuping REN[10], Lijuan CAO[21], Yayang LU[22], Juan DU[1], Kewei LYU[23], Albertus SULAIMAN[24], Michael MAYER[25,26], Huizan WANG[27], Zhanhong MA[27], Senliang BAO[27], Henqian YAN[27], Zenghong LIU[28], Chunxue YANG[7], Xu LIU[11], Zeke HAUSFATHER[29], Tanguy SZEKELY[30], and Flora GUES[31]

[1]*National Key Laboratory of Earth System Numerical Modeling and Application*, *Institute of Atmospheric Physics*, *Chinese Academy of Sciences*, *Beijing* 100029, *China*

[2]*University of St. Thomas*, *School of Engineering*, *Minnesota* 55105, *USA*

[3]*NSF National Center for Atmospheric Research*, *Boulder*, *Colorado* 80307, *USA*

[4]*University of Auckland*, *Auckland* 0630, *New Zealand*

[5]*National Oceanic and Atmospheric Administration*, *National Centers for Environmental Information*, *Silver Spring*, *Maryland* 20910, *USA*

[6]*National Oceanic and Atmospheric Administration*, *National Centers for Environmental Information*, *Asheville*, *NC* 28801, *USA*

[7]*National Research Council (CNR) Institute of Marine Sciences (ISMAR)*, *Rome* 00133, *Italy*

[8]*Mercator Ocean International*, *Toulouse* 31400, *France*

[9]*Department of Earth and Environmental Science*, *University of Pennsylvania*, *Philadelphia*, *Pennsylvania* 19104, *USA*

[10]*Institute of Oceanology*, *Chinese Academy of Sciences*, *Qingdao* 266071, *China*

[11]*National Marine Environmental Forecasting Center*, *Ministry of Natural Resources of China*, *Beijing* 100081, *China*

[12]*North Carolina Institute for Climate Studies (NCICS)*, *North Carolina State University*, *Asheville*, *NC* 28804, *USA*

[13]*Oceanographic Data Center*, *Chinese Academy of Sciences*, *Qingdao* 266071, *China*

[14]*College of Oceanography*, *Hohai University*, *Nanjing* 210098, *China*

[15]*National Marine Data and Information Service*, *Tianjin* 300171, *China*

[16]*Istituto Nazionale di Geofisica e Vulcanologia*, *Sede di Bologna*, *Bologna* 40128, *Italy*

[17]*South China Sea Institute of Oceanology*, *Chinese Academy of Sciences*, *Guangzhou* 510301, *China*

[18]*ESSIC/CISESS-MD*, *University of Maryland*, *College Park*, *MD* 20740, *USA*

[19]*Computer Network Information Center*, *Chinese Academy of Sciences*, *Beijing* 100083, *China*

[20]*Eco-Environmental Monitoring and Research Center*, *Pearl River Valley and South China Sea Ecology and Environment Administration*, *Ministry of Ecology and Environment*, *Guangzhou* 510611, *China*

[21]*National Meteorological Information Center*, *China Meteorological Administration*, *Beijing* 100081, *China*

[22]*International Research Center of Big Data for Sustainable Development Goals*, *Beijing* 100094, *China*

[23]*Xiamen University*, *Xiamen* 361005, *China*

[24]*Research Center for Climate and Atmosphere*, *National Research and Innovation Agency (BRIN)*, 40173, *Indonesia*

[25]*Research Department*, *European Centre for Medium-Range Weather Forecasts*, *Reading RG2 9AX*, *UK*

[26]*Department of Meteorology and Geophysics*, *University of Vienna*, *Vienna* 1090, *Austria*

[27]*College of Meteorology and Oceanography*, *National University of Defense Technology*, *Changsha* 410073, *China*

[28]*State Key Laboratory of Satellite Ocean Environment Dynamics*, *Second Institute of Oceanography*,

* Corresponding author: Lijing CHENG
Email: chenglij@mail.iap.ac.cn

Ministry of Natural Resources, *Hangzhou* 310012, *China*
[29]*Stripe*, *Inc.*, *South San Francisco*, *CA* 94080, *USA*
[30]*Ocean Scope*, *Brest* 29200, *France*
[31]*CELAD*, *Balma* 31130, *France*

(Received 24 December 2024; revised 7 January 2025; accepted 8 January 2025)

ABSTRACT

Heating in the ocean has continued in 2024 in response to increased greenhouse gas concentrations in the atmosphere, despite the transition from an El Niño to neutral conditions. In 2024, both global sea surface temperature (SST) and upper 2000 m ocean heat content (OHC) reached unprecedented highs in the historical record. The 0–2000 m OHC in 2024 exceeded that of 2023 by 16 ± 8 ZJ (1 Zetta Joules = 10^{21} Joules, with a 95% confidence interval) (IAP/CAS data), which is confirmed by two other data products: 18 ± 7 ZJ (CIGAR-RT reanalysis data) and 40 ± 31 ZJ (Copernicus Marine data, updated to November 2024). The Indian Ocean, tropical Atlantic, Mediterranean Sea, North Atlantic, North Pacific, and Southern Ocean also experienced record-high OHC values in 2024. The global SST continued its record-high values from 2023 into the first half of 2024, and declined slightly in the second half of 2024, resulting in an annual mean of 0.61°C ± 0.02°C (IAP/CAS data) above the 1981–2010 baseline, slightly higher than the 2023 annual-mean value (by 0.07°C ± 0.02°C for IAP/CAS, 0.05°C ± 0.02°C for NOAA/NCEI, and 0.06°C ± 0.11°C for Copernicus Marine). The record-high values of 2024 SST and OHC continue to indicate unabated trends of global heating.

Key words: ocean heat content, sea surface temperature, ocean temperature, global warming, climate

Citation: Cheng L. J., and Coauthors, 2025: Record high temperatures in the ocean in 2024. *Adv. Atmos. Sci.*, https://doi.org/10.1007/s00376-025-4541-3.

Article Highlights:

- In 2024, the global upper 2000 m ocean heat content was the highest ever recorded by modern instruments, ~16 ZJ higher than the 2023 value.
- The 2024 annual mean global SST was 0.05°C–0.07°C higher than in 2023, and a new record for the instrumentation era.
- Regions with record-high OHC in 2024 included the Indian Ocean, tropical Atlantic, Mediterranean Sea, North Atlantic, North Pacific, and Southern Ocean.

1. Ocean and climate changes over the past year

The year 2024 marks another in a series of years characterized by record-breaking changes in Earth's climate system and widespread anomalous weather patterns, indicative of the planet's continued warming. The global climate continues to transit into uncharted territory (e.g., Rahmstorf, 2024). Each of the first seven months of 2024 set new global mean surface temperature (GMST) records, extending a remarkable streak of 13 consecutive record-breaking months dating back to 2023, based on Berkeley (Rohde and Hausfather, 2020) and ERA5 (Hersbach et al., 2023) data. The warming has been observed globally, with 63 countries experiencing their hottest boreal summer on record. Over 2024, a staggering 104 countries have recorded their hottest temperatures ever (Berkeley GMST). The Antarctic sea-ice extent for much of early 2024 was at the low end of the historical 1979–2010 range, similar to that experienced in 2023.

Climate change often amplifies natural weather and climate phenomena, intensifying their severity and causing extreme events to become more widespread globally (IPCC, 2023). Drought, flooding, crop failure, heatwaves, and wildfires became common in many areas of the world in 2024, in southern Africa in February, southern Asia and the Philippines in April, heatwaves and rainstorms in South China in summer, the Pantanal in Brazil in June, widespread heatwaves and wildfires in Europe in August, floods in Chad, Nigeria and Central Europe in September, and in the northeast United States in November (Copernicus Climate Change Service). In the United States, Hurricane Helene caused devastating flooding in the Southeast, resulting in over 200 deaths and billions of dollars of economic losses. In China, since 1961, the summer air temperature reached its highest value, accompanied by the most intense rainstorms from the southeast to the northeast regions.

All these changes and extreme events are directly or indirectly impacted by human-induced climate change (IPCC, 2021, 2023; Seneviratne et al., 2021). Human activities release greenhouse gases (GHGs) into the atmosphere, increasing their concentration and trapping heat within the climate system, which drives global heating. CO_2, a major GHG, reached an annual average concentration of more than 420 ppm in the atmosphere in 2024 (Forster et al., 2024), which is a record-high level in at least 2 million years (IPCC, 2021), and ~140 ppm higher than the pre-industrial level of around 280 ppm (Friedlingstein et al., 2023). Other changes in water vapor, clouds, and atmospheric aerosols compound the excess heating (IPCC, 2021). Internal variability linked to ENSO (El Niño–Southern Oscillation)

and PDO (Pacific Decadal Oscillation) drive additional variations.

About 90% of the heat accumulated in the climate system is stored in the ocean, increasing ocean temperatures and ocean heat content (OHC) (Hansen et al., 2011; Von Schuckmann et al., 2020, 2023; Abraham et al., 2022; Cheng et al. 2022a). Thus, OHC is a key climate indicator for monitoring planetary warming. Due to the ocean's large heat capacity and immense volume, the change in OHC is characterized by much smaller month-to-month and year-to-year fluctuations as compared to the surface temperature, making OHC a robust metric of climate change (Cheng et al., 2017b; Cheng et al. 2022a).

The GMST change is one of the key metrics for global climate action efforts, together with OHC, and sea level rise. GMST, and hence sea surface temperature (SST), are critical because they are crucial for climate feedback (e.g., blackbody radiation and cloud feedback) and also drive many climate impacts (e.g., storms and wildfires) (e.g., Zhang et al. 2020; Armour et al., 2024; Gilford et al., 2024; Hu et al., 2024). The Paris Agreement, signed by 196 parties at the 2015 United Nations Climate Change Conference, set a goal of limiting global temperature increases to well below 2°C, while pursuing efforts to limit the increase to 1.5°C. However, there was a notable increase in global SST and GMST from 2022 to 2023: ~0.24°C for SST and ~0.29°C for GMST. This increase led to an annual mean GMST level of 1.4°C–1.5°C above the pre-industrial level (Forster et al., 2024). Now, 2024 exceeds those values (see below). Regional SST hotspots are associated with marine heatwaves and have major consequences for marine life (Smith et al., 2023). The detailed causes of this year-to-year spike are still debated, but possible reasons include ENSO, less negative aerosol forcing, a record-low planetary albedo, and GHG-forced changes that include changes in the atmosphere and ocean circulation (e.g., Kuhlbrodt et al., 2024; Raghuraman et al., 2024; Schmidt, 2024; Goessling et al., 2025).

To provide climate information and better serve climate actions, this study updates the OHC and SST through 2024 and analyzes their global and regional changes based on multiple datasets from major international data centers. The data and processing are introduced in section 2, followed by a global analysis in section 3. The spatial distributions of OHC and SST anomalies are presented in sections 4 and 5, respectively, and in section 6 for OHC regional changes. The consequences and implications of the observed 2024 changes are discussed in section 7.

2. Advances in data and processing

2.1. *Data*

The OHC estimates are based on two gridded observational products and an ocean reanalysis product. The observational products include: (i) the Institute of Atmospheric Physics (IAP) at the Chinese Academy of Sciences (CAS) (Cheng et al., 2017a, 2024a; Zhang et al. 2024); and (ii) Copernicus Marine (von Schuckmann & Le Traon, 2011). For the IAP/CAS product, the primary source data are obtained from in situ measurements made available through the World Ocean Database (WOD) (Boyer et al., 2018, Mishonov et al., 2024a), where all instrumental data are used. The IAP/CAS dataset also uses real-time Argo data from the Observation and Research Station of Global Ocean Argo System (Hangzhou). The IAP/CAS dataset is a monthly gridded product with a 1° × 1° horizontal resolution, and covers the ocean's upper 6000 m. In 2024, there were some modifications to the data sources and data processing techniques for the IAP/CAS product, which led to some changes in OHC/SST values compared with the previous year's release (Cheng et al. 2024b). The changes are designed to incorporate more data and improve infilling methods and include the following:

(1) More in situ observations are incorporated into the IAP/CAS analysis, comprising 89 716 profiles that are not included in WOD. These additional data are mainly distributed in the Northwest Pacific Ocean, Indonesian Throughflow regions, seas around China, and the Arctic after the 1980s.

(2) There is an update to the quality control (QC) procedure (CODC-QC; Tan et al., 2023) in the IAP/CAS analysis, with additional QC. The latter applies an iterative vertical gradient check and an iterative spike check to each QC-ed profile until no further measurements are flagged.

(3) The climatology used in the IAP/CAS analysis has been reconstructed and updated based on the updated QC procedure.

(4) Biases in ocean temperature profiles obtained by satellite relay data loggers and time-depth recorders attached to marine mammals have been corrected following Gouretski et al. (2024). This implementation impacts the OHC in the polar regions from ~2005 to the present.

(5) The bias correction scheme for Nansen Bottle (BOT) data has also been updated (Gouretski et al., 2022). Here, only standard level BOT data have been corrected, while in previous versions, we corrected all bottle data with low resolution. Thus, the new correction is more conservative, leading to slightly weaker OHC trends from the 1950s to ~1980.

For the Copernicus Marine data, only Argo data are used for the period 2005–2024 and are based on a simple box averaging scheme using a weighted mean applied on an irregular observation field (von Schuckmann and Le Traon, 2011). Uncertainties in the Copernicus Marine data include data processing methods and the choice of climatology. Non-gridded in situ observations of the subsurface temperature from the Copernicus Marine product CORA are used as inputs of the Copernicus Marine OHC data (EU Copernicus Marine, 2023a; Szekely et al., 2024).

The global reanalysis dataset is CIGAR (CNR ISMAR Global historical Reanalysis; Storto and Yang, 2024) developed at the National Research Council of Italy, which is based on the Nucleus for European Modelling of the Ocean

(NEMO)-SI^3 ocean and sea-ice model (version 4.0.7; Madec et al., 2017) implemented at a horizontal resolution of about 1°, with enhanced meridional resolution in the tropics [up to (1/3°)], and 75 vertical depth levels with partial steps (Banier et al., 2012). The model is forced at the surface by the ECMWF ERA5 reanalysis (Hersbach et al., 2020) and includes daily-varying freshwater discharge from land sourced from the Japan Meteorological Agency's JRA-55-do (Japanese 55-year Reanalysis: surface dataset for driving ocean-sea ice models) (Tsujino et al., 2018). A three-dimensional variational data assimilation scheme (Storto et al., 2018) with nonlinear QC of observations (Storto, 2016) is adopted to ingest all in situ observations from the EN4 dataset (Good et al., 2013). Additionally, surface relaxation to COBEv2 SST observations (Ishii et al., 2005) and a large-scale model bias correction scheme (Storto et al., 2016) complete the reanalysis system. The dataset presented here is a real-time extension of the ensemble CIGAR system (Storto and Yang, 2024), called CIGAR–RT, where only four members (out of the 32) are updated in real time, and Argo data ingested directly from the Coriolis/Ifremer Argo Global Data Assembly Centers (GDAC) replace the EN4 dataset for December 2024. These four members differ in the bulk formulas used for the air–sea flux calculation, the MBT and XBT bias corrections applied within the EN4 dataset, and the data assimilation configuration, as detailed in Storto and Yang (2024).

Additional regional reanalysis data (Escudier et al., 2021; Nigam et al., 2021) (CMS-MEDREA) are used to assess the Mediterranean OHC change. CMS-MEDREA assimilated XBT, CTD, and Argo profiles, integrating data from CMS and SeaDataNet (https://www.seadatanet.org/) and CMS satellite along-track sea level anomalies (Escudier et al., 2020, 2021). This product is generated by a numerical system composed of a hydrodynamic model supplied by NEMO and a variational data assimilation scheme. The model horizontal grid resolution is (1/24°) (about 4–5 km), with 141 unevenly spaced vertical levels.

The SSTs in this study are based on three products: (1) the first layer (1 m) of the IAP/CAS gridded product; (2) the Extended Reconstructed Sea Surface Temperature (ERSST) dataset, which is a global monthly SST dataset on a 2° × 2° grid from January 1854 to the present (Huang et al. 2017; 2020); and (3) the Copernicus Marine (OSTIA, Good et al., 2020; EU Copernicus Marine, 2023b, 2023c) global SST reprocessed product from 1982 to the present.

The data sources of the latest version (version 5) of ERSST (ERSST.v5) include observations from ships and buoys from the International Comprehensive Ocean–Atmosphere Data Set (ICOADS) Release 3.0.2, Argo floats above 5 m depth, and the Hadley Centre Ice-SST version 2 (HadISST2) ice concentration. ERSST.v5 has improved SST spatial and temporal variability by (a) reducing spatial filtering in training the reconstruction functions of the 140 empirical orthogonal teleconnections (EOTs), (b) removing high-latitude damping in EOTs, (c) adding 10 more EOTs in the Arctic, (d) using NMAT (nighttime marine air temperature) before 1985 and buoy-SST after 1985 as a reference in correcting ship SST biases, and (e) using an unadjusted first-guess instead of an adjusted first-guess in QC.

The Copernicus Marine product (OSTIA) provides daily gap-free maps of Foundation SST and ice concentration (referred to as an L4 product) on a 0.05° × 0.05° horizontal spatial grid resolution by using in situ and satellite data. This product provides the Foundation SST, with the temperature diurnal variability removed (Good et al., 2020).

Finally, we note that near real-time updates of the climate datasets and time series put additional constraints on the data generators, as operationalizing the climate records means handling real-time data, the quality of which is always not guaranteed. In future, we will explore the possibility to include more datasets if available.

2.2. *Trend and uncertainty calculation*

The trends in this study have been estimated by the LOWESS approach (Cheng et al. 2022b), i.e., we apply a locally weighted scatterplot smoothing (LOWESS) to the OHC time series (25-year window, equal to an effective 15-year smoothing), and then the OHC difference between the first and the end year is used to calculate the rate. The trend uncertainty also follows the LOWESS approach based on a Monte Carlo simulation and calculating ± 1.9 times the standard deviation (95% confidence interval) of 1000 rate values.

3. The global ocean state in 2024

3.1. *OHC*

The global OHC changes within the upper 2000 m ocean layer since 1958 (Fig. 1) show that there has been an unequivocal ocean warming trend in recent decades, regardless of the data sources and processing techniques. The upper 2000 m of the world's ocean has warmed on average by 6.4 ± 0.3 ZJ yr^{-1} during 1958–2024 (IAP/CAS) (Fig. 1a). The 95% confidence levels are calculated using the approach of Cheng et al. (2022b) (Section 2.2). There has been a two- to threefold increase in the rate of OHC since the late 1980s. For example, according to the IAP analysis, the OHC trend for 1958–1985 is 2.9 ± 0.5 ZJ yr^{-1}, and since 1986 the OHC trend is roughly three times as large: 9.0 ± 0.5 ZJ yr^{-1} (Fig. 1). Since 2007, the upper 2000 m ocean warming rate has been 11.1 ± 1.1 ZJ yr^{-1}, 10.1 ± 1.2 ZJ yr^{-1}, 12.3 ± 2.0 ZJ yr^{-1} for the IAP/CAS, Copernicus Marine, CIGAR-RT datasets respectively. The increase in the OHC rate in recent decades indicates a multidecadal acceleration of ocean warming (Cheng et al. 2019a, 2024a; Loeb et al., 2021; Minière et al. 2023; Storto and Yang, 2024). Consistency among these datasets in the past two decades indicates the robustness of the ocean warming trends. For all datasets, the uncertainty of the OHC estimates has been reduced in more recent periods (green bars in Fig. 1), because of improvements in the global ocean observing system

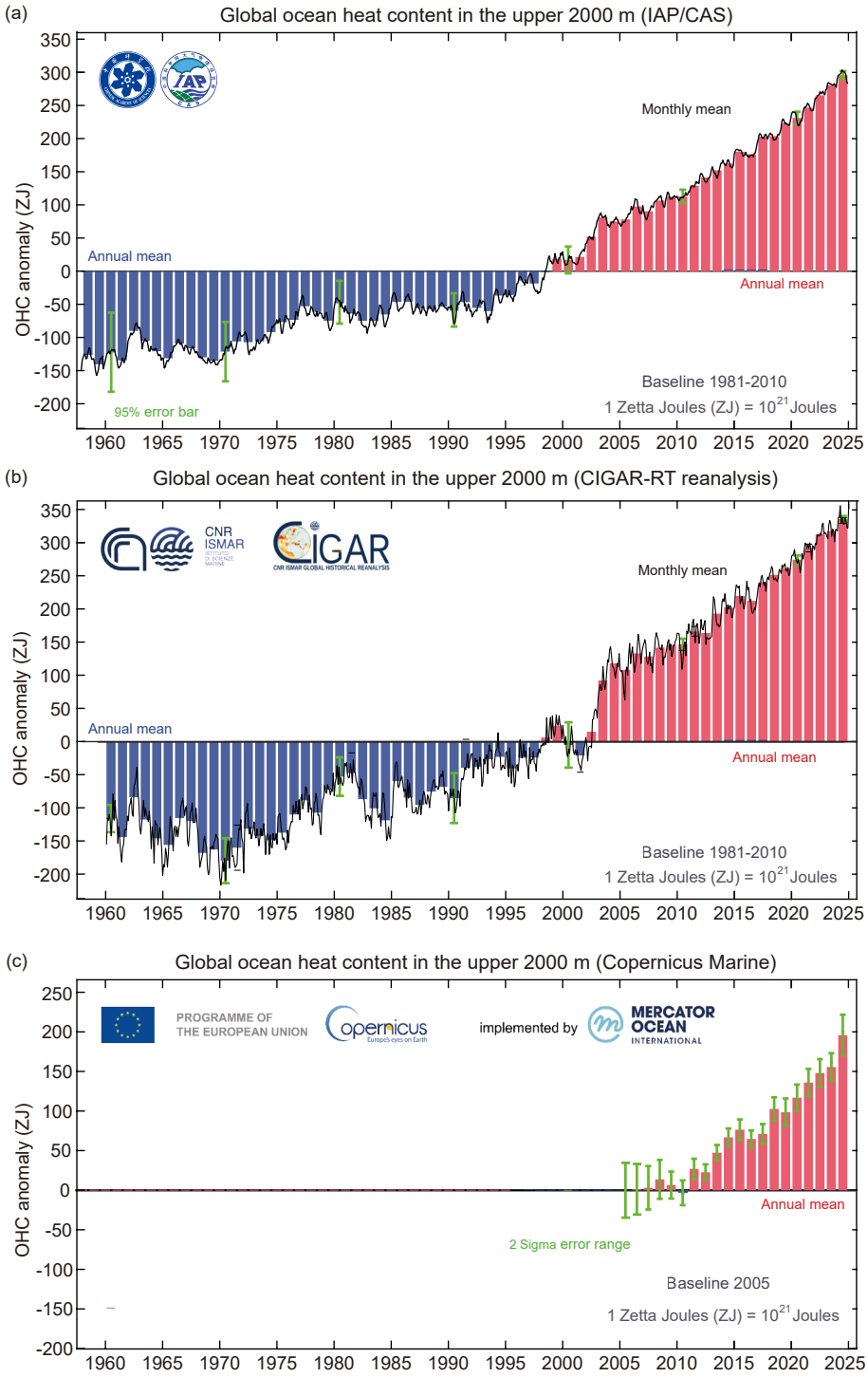

Fig. 1. Global upper 2000 m OHC from 1958 through 2024 according to (a) IAP/CAS, (b) CIGAR-RT, and (c) Copernicus Marine (1 ZJ = 10^{21} J). The black line in (a, b) shows monthly values, and the histogram presents annual anomalies. The time series are relative to the 1981–2010 baseline for IAP/CAS and CIGAR-RT data, and the 2005 baseline for the Copernicus Marine data. The 2005 values for IAP/CAS and CIGAR-RT data are 78 ZJ and 108 ZJ relative to the 1981–2010 baseline, respectively. The green bars indicate the uncertainty estimates from different datasets.

(notably Argo) in terms of better data quality and coverage.

The 2024 upper 2000 m OHC exceeds the 2023 value by 16 ± 8 ZJ (IAP/CAS), 18 ± 7 ZJ (CIGAR-RT), and 40 ± 31 ZJ (Copernicus Marine, updated to November 2024), making 2024 the hottest year on record for OHC (Figs. 1 and 2, Table 1). A preliminary result from NCEI/NOAA data (Levi-

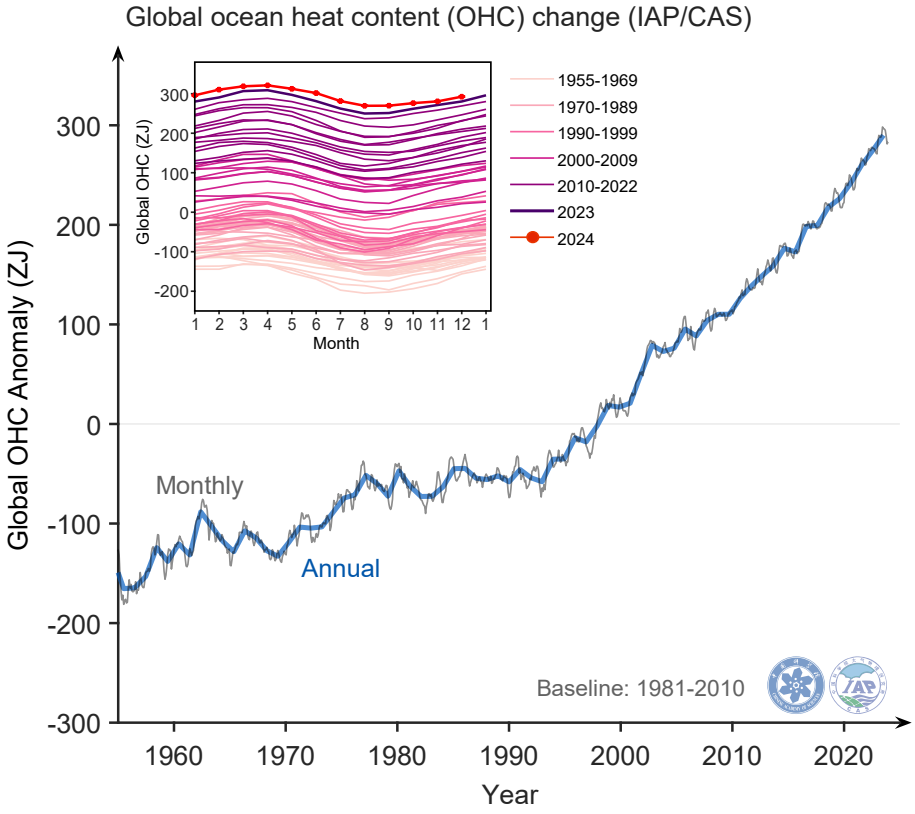

Fig. 2. Global upper 2000 m OHC changes from 1955 through 2024 (units: ZJ). The thick lines are the annual values, and the thin lines are the monthly values. The anomalies are relative to a 1981–2010 baseline. The within-year variation of OHC is shown in the inner box, with 2024 values shown in red.

Table 1. Ranked order of the five hottest years of the world's oceans since 1955. The OHC values are for the upper 2000 m in units of ZJ, relative to the 1981–2010 average. Note that the IAP/CAS values from 2020 to 2023 are about 6–8 ZJ lower than the previous release [Table 1 in Cheng et al. (2024b)] because of the update to the Nansen Bottle bias correction that leads to a slightly higher IAP/CAS 1981–2010 baseline. The update to the QC and climatology construction methods are responsible for differences of about 0–2 ZJ in these values. These changes do not impact recent year-to-year increases.

Rank	Year	OHC (IAP/CAS) (units: ZJ)	OHC (CIGAR-RT) (units: ZJ)
1	2024	297	336
2	2023	281	318
3	2022	265	313
4	2021	246	292
5	2020	231	275

tus et al,. 2012) indicates an increase of 12 ZJ (subject to change after further quality control) from 2023 to 2024 for the upper 2000 m OHC, confirming that 2024 is another record year. The magnitude of the increase varies, mainly because the data sources and data processing differ (including QC, bias correction, climatology choice, and mapping); see Boyer et al. (2016) and Cheng et al. (2022a) for detailed discussion. However, the OHC increase is within the uncertainty range and all the datasets show that the past five consecutive years have been the warmest on record. The increase in OHC is compatible with changes in Earth energy imbalance (EEI) from CERES (Loeb et al., 2021, Cheng et al., 2024a).

Besides the long-term trend, the global OHC generally peaks shortly before, and then declines around, an El Niño event, associated with ocean heat release into the atmosphere, mainly through increased evaporation and thus realized in the atmosphere as latent heating in precipitation, which drives teleconnections (Trenberth et al. 2002; Roemmich and Gilson, 2011; Cheng et al., 2019b)—as can be seen, for example, with the 2015/16 El Niño event (Mayer et al., 2018). The ENSO perturbation on the global OHC is generally within ± 10 ZJ, and a slightly lower OHC value than the previous year is expected after an El Niño event (Cheng et al., 2019). In 2024, OHC anomalies increased for the first eight months (the January–August average was ~20 ZJ higher than the 2023 mean) and decreased from August to December (Figs. 1 and 2). This OHC evolution is consistent with El Niño ocean heat loss effects combined with anthropogenic global heating.

3.2. *SST*

The global SST also shows a significant increase since at least the 1950s (Fig. 3). The mean SST trend is 0.12°C ±

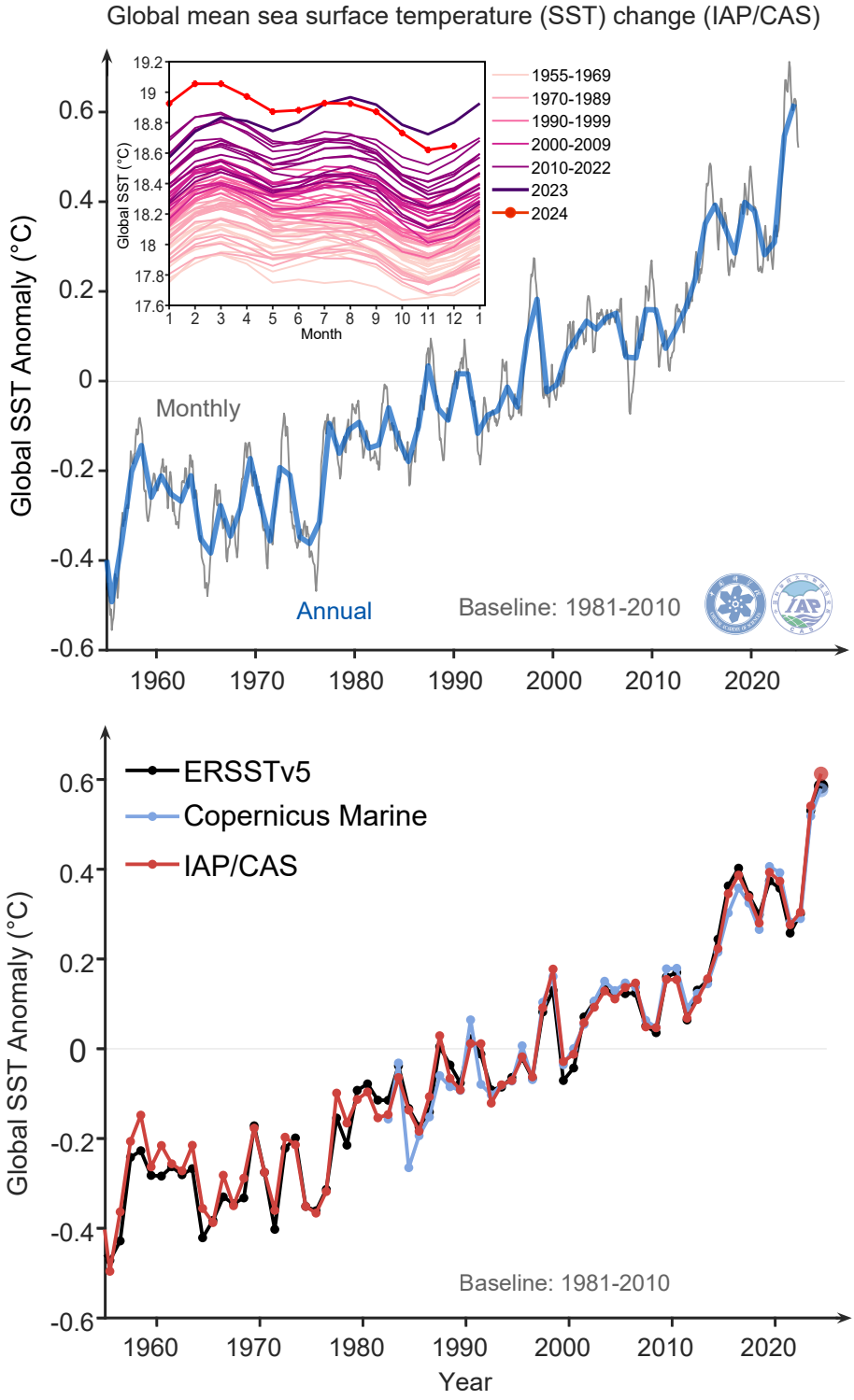

Fig. 3. Global SST changes from 1955 through 2024 (units °C). Upper panel: The thick lines are the annual values, and the thin lines are the monthly values. The anomalies are relative to a 1981–2010 baseline. The within-year variation of SST is shown in the inner box, with 2024 values shown in red. Lower panel: Global annual mean SST changes from three data products (ERSST, Copernicus Marine, and IAP/CAS).

0.01°C (10 yr)$^{-1}$ for both IAP/CAS and ERSST data since 1958. Regridded satellite data (OSTIA from Copernicus Marine) indicate a warming rate of 0.15°C ± 0.02°C (10 yr)$^{-1}$ since 1982, consistent with other in situ observation-based results during the same period. The relative year-to-year fluctuations are much more intense for SST than the OHC record (Fig. 3 versus Figs. 1 and 2).

A sharp SST increase occurred in 2023; the annual

mean 2023 SST was 0.24°C ± 0.02°C higher than in 2022 (Fig. 3, IAP/CAS) (Raghuraman et al., 2024). This is the highest annual increase on record, with the second largest jump of 0.22°C occurring from 1976 to 1977, which also accompanied a La Niña–El Niño transition. The record-high SST anomalies started from April 2023 and continued to July 2024, and the 2024 SST became the highest on record during the end phase of the El Niño event. In the second half of 2024, the global SST started to decrease relative to the 2023 value, with the transition to a neutral ENSO phase (Fig. 3). The annual mean 2024 SST is an astounding 0.61°C ± 0.02°C (IAP/CAS) higher than the 1981–2010 average (0.58°C ± 0.02°C for ERSST, 0.58°C ± 0.07°C for Copernicus Marine) (Fig. 3). Compared to the 2023 value, the 2024 SST is 0.07°C ± 0.02°C higher for IAP/CAS data (Fig. 3; 0.05°C ± 0.02°C and 0.06°C ± 0.11°C for ERSST and Copernicus Marine, respectively) (Table 2).

4. Spatial patterns of OHC changes in 2024

Spatial maps of the 2024 OHC anomaly relative to the mean 1981–2010 conditions (Fig. 4) reveal patterns of long-term ocean warming trends. Most of the ocean has warmed profoundly, with some areas (much of the Atlantic, North Pacific, West Indian, the Mediterranean Sea, and northern parts of the Southern Ocean) warming faster than the global mean (Figs. 4 and 5). The northern flank of the Antarctic Circumpolar Current (ACC) shows the most intense and deep-reaching ocean warming (Figs. 4 and 5), and acts as a key region of ocean heat uptake from which heat is transported northward by the ocean before it converges in the downwelling-dominated regions north of the ACC (Armour et al., 2016; Cai et al., 2023). The Atlantic basin shows stronger and deeper-reaching area-averaged OHC change than the Indian and Pacific basins, likely because the heat was transported out of the Indo-Pacific into the Atlantic basin (Cheng et al. 2022a, Mishonov et al., 2024b) and enhanced heat uptake in the Atlantic Ocean associated with changes in atmospheric circulation and aerosols (Grist et al., 2010; McMonigal et al., 2023; Ren et al., 2024). The cooling trends in the subsurface tropical and subtropical regions of the Pacific and Indian basins (Figs. 4 and 5) can be linked to the acceleration of the wind-driven ocean circulation (Qu et al. 2019; Hu et al. 2020), which leads to increased low-latitude upwelling and cooling and freshening of major intermediate water masses (except in the South Atlantic) (Wong et al. 1999; Durack and Wijffels 2010; Jiang et al., 2024) (Figs. 4 and 5). Detailed discussion on the long-term OHC trend patterns is provided in the review by Cheng et al. (2022a).

Compared with the year 2023, the 2024 OHC shows a cooling band along the equator in the Pacific Ocean (minimum < −3 GJ m^{-2}, 1 GJ = 10^9 J) and warming in the subtropical regions in both hemispheres (maximum > 2 GJ m^{-2}) (Fig. 6), indicating that heat is discharged from the equatorial

Table 2. Ranked order of the five hottest years of the global mean SST anomaly since 1955 (Since 1981 for Copernicus Marine data), relative to the 1981–2010 baseline.

Rank	Year	SST anomaly (IAP/CAS) (units: °C)	SST anomaly (ERSST5) (units: °C)	SST anomaly (Copernicus Marine) (units: °C)
1	2024	0.61	0.58	0.58
2	2023	0.54	0.53	0.52
3	2019	0.39	0.37	0.40
4	2016	0.38	0.40	0.36
5	2020	0.37	0.36	0.39

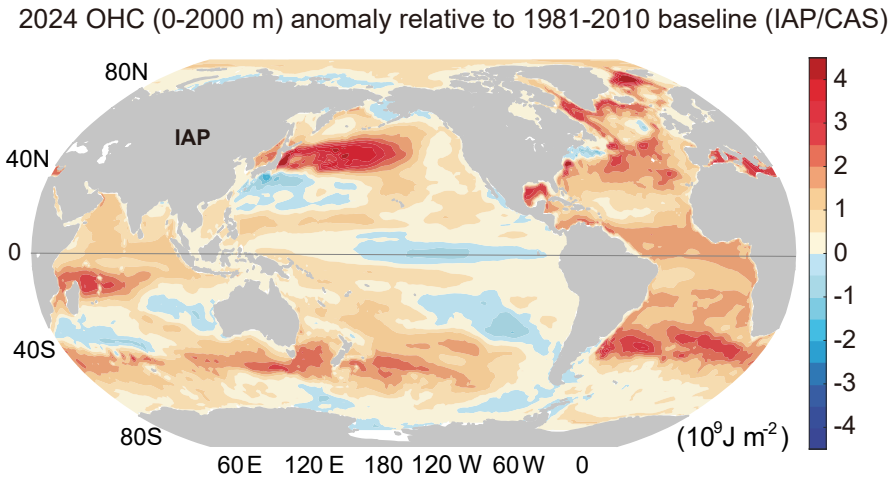

Fig. 4. The annual OHC anomaly in 2024 relative to a 1981–2010 baseline for the IAP/CAS data; units: 10^9 J m^{-2} [data updated from Cheng et al. (2024a)].

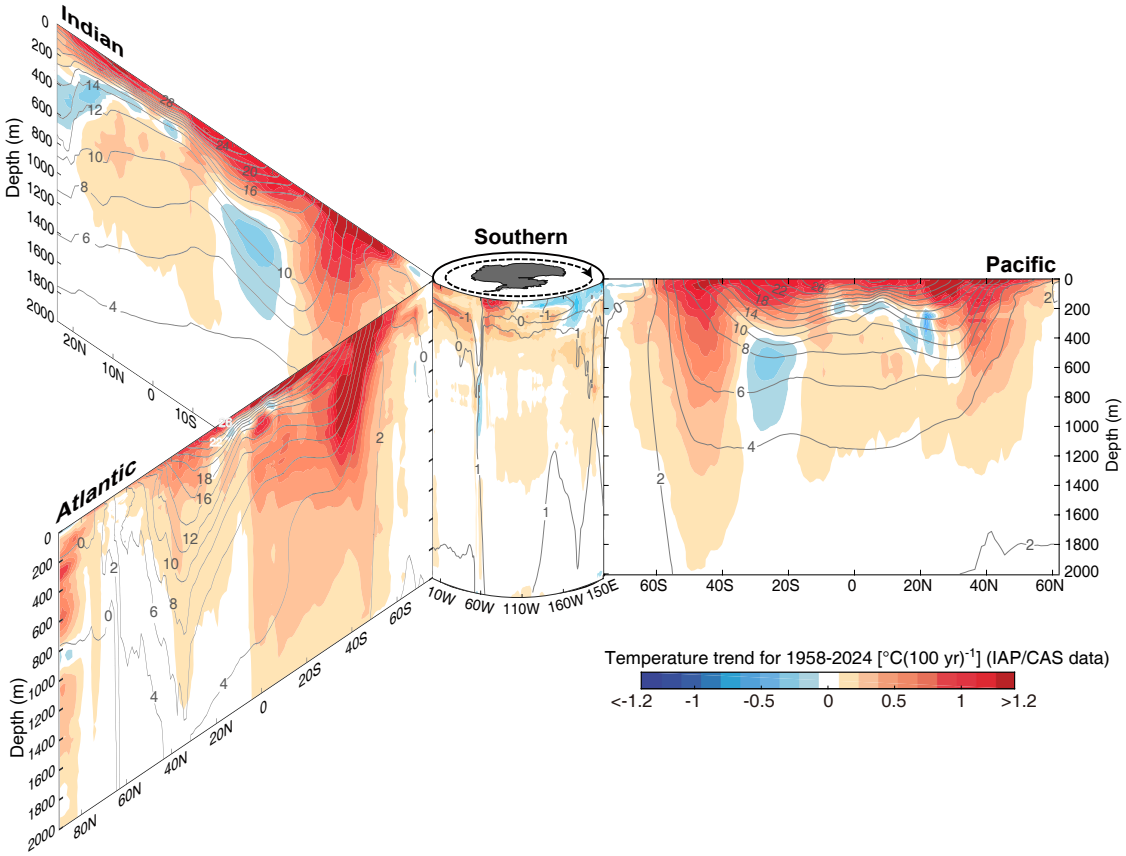

Fig. 5. Vertical section of the zonal mean ocean temperature trends within 1958 to 2024 from the sea surface to 2000 m. The trends are calculated using the LOWESS approach (Cheng et al., 2022b) with a span width of 25 years (the effective time scale is ~15 years). Shown are the zonal mean sections in each ocean basin organized around the Southern Ocean (south of 60°S) in the center. Black contours show the associated climatological mean temperature with intervals of 2°C (in the Southern Ocean, 1°C contour intervals are used) [data updated from Cheng et al. (2024a)].

regions into the subtropics (Cheng et al., 2019b). This is consistent with the "recharge–discharge oscillator" paradigm, which is one proposed mechanism for ENSO formation (Cane and Zebiak 1985). Strong warming anomalies are manifested at about 40°N in the central North Pacific Ocean (maximum ~2 GJ m^{-2}, Fig. 6). The Atlantic Ocean shows warm anomalies at low latitudes and cool anomalies along 40°S and 40°N, a typical response pattern of the Atlantic Ocean to ENSO [see Fig. 2 of Cheng et al. (2019b)].

The Indian Ocean shows warm anomalies in the tropical band (maximum > 2 GJ m^{-2}) and cold anomalies south of 10°S (minimum < −1 GJ m^{-2}) (Fig. 6)—a pattern characterizing the lagged response to the 2023–2024 El Niño. For example, the enhanced warming of the southwestern tropical Indian Ocean is caused by anticyclonic wind anomalies generated through El Niño's atmospheric teleconnections (Xie et al., 2002). Upwelling waves in the western tropical Pacific during El Niño can propagate into the southeastern Indian Ocean through the Indonesian Seas and cause cooling anomalies there (Cai et al., 2005; Li et al., 2020) in association with a weakened Indonesian Throughflow (ITF, Mayer et al., 2014).

5. Spatial patterns of SST changes in 2024

The spatial pattern of SST change (2024 SST relative to a 1981–2010 baseline) (Fig. 7) is distinct from the upper 2000 m OHC (Fig. 4). This pattern mainly reflects the SST changes over the past three decades, showing a widespread ocean surface warming in most ocean areas. The long-term SST increase is mainly driven by GHG forcing (Bindoff et al., 2019). The SST increase is stronger in the Northern Hemisphere than in the Southern Hemisphere (von Schuckmann et al., 2024). The relative warming of the Northern Hemisphere may be linked to the abatement of industrial aerosol emissions by China since ~2010 and regulation of shipping sulfur emissions (Wang et al., 2023; Yoshioka et al., 2024). The warmest sea surface anomalies occur around 40°N in the Northwest Pacific Ocean (with maximum anomalies >3°C) and North Atlantic Ocean (maximum > 2°C), consistent with OHC (Fig. 7 compared with Fig. 4). Some regions of the Southern Ocean show cold anomalies (Fig. 7). Multiple hypotheses have been proposed to explain recent cooling trends, including the freshwater input from Antarctic ice-sheet melt, northward sea-ice transport, and Southern Ocean natural variability (Dong et al., 2023; Simp-

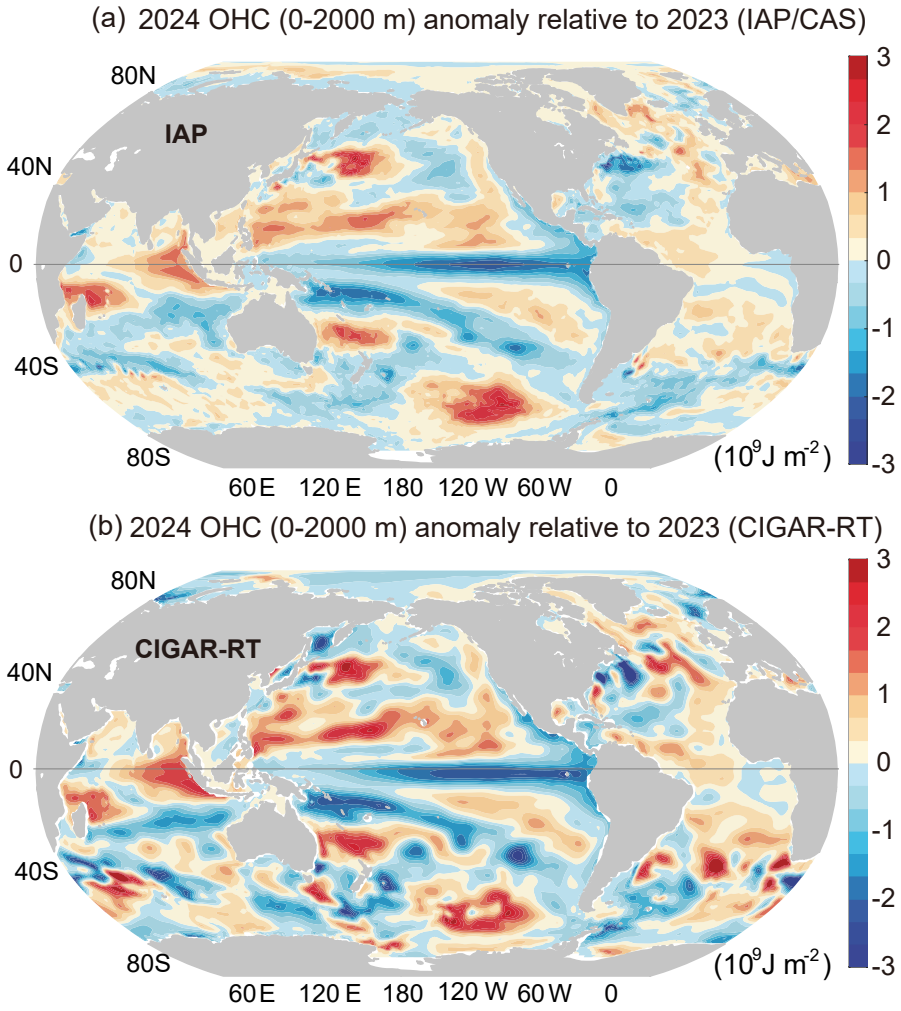

Fig. 6. Differences of annual mean upper 2000 m OHC values between 2024 and 2023, based on (a) IAP/CAS analysis and (b) CIGAR-RT . Units: 10^9 J m^{-2} [data updated from Cheng et al. (2024a)].

kins et al., 2024).

The 2024–23 difference in the SST pattern (Fig. 8) reveals strong cooling (< −2°C) in the middle and eastern part of the Pacific Ocean, associated with warming in the western Pacific, tropical Indian, and Atlantic ocean basins (with a maximum of 1°C). This pattern is likely associated with the strengthening of the tropical trade winds after El Niño, which triggers ocean waves and thermocline feedback, causing strengthened upwelling and SST cooling in the eastern Pacific Ocean. The changes of the thermocline and Hadley and Walker circulation are likely to be key drivers of the Indian and Atlantic ocean changes (Cheng et al. 2019b).

There are regions of warming in the Southern Ocean within 35°–70°S and 180°–60°W with maximum SST increases of ~2°C from 2023 to 2024 (Fig. 8). Such changes are also reflected in the OHC changes (Fig. 6, ~3 GJ m^{-2}), indicating that the warm anomalies penetrate into the ocean interior, marking a key region of ocean heat uptake in 2024.

6. Regional OHC changes in 2024

Regional OHC changes reveal the impacts of both anthropogenically forced long-term changes and variability from interannual to decadal scales (Fig. 9). Six out of the eight ocean regions investigated in Fig. 9, including the Indian Ocean, tropical Atlantic, Mediterranean Sea, North Atlantic, North Pacific, and Southern Ocean, show record-high OHC values in 2024.

The Indian Ocean shows a sharp OHC increase from 2023 to 2024, with a 10.3 ZJ (0.35 GJ m^{-2}) increase from 2023 to 2024 (Fig. 9). A similar magnitude of increase occurs from 2018 to 2019 (Fig. 9), followed by a big OHC decrease from 2020 to 2022. These substantial interannual fluctuations result partly from the El Niño that matured in 2023–2024 (and 2019) that drove a basin-scale warming of the tropical Indian Ocean through teleconnections on surface winds and cloud cover (Trenberth and Zhang 2019) and changes in the ITF. Both atmospheric and oceanic processes impact the Indian Ocean energy budget (Mayer et al. 2014).

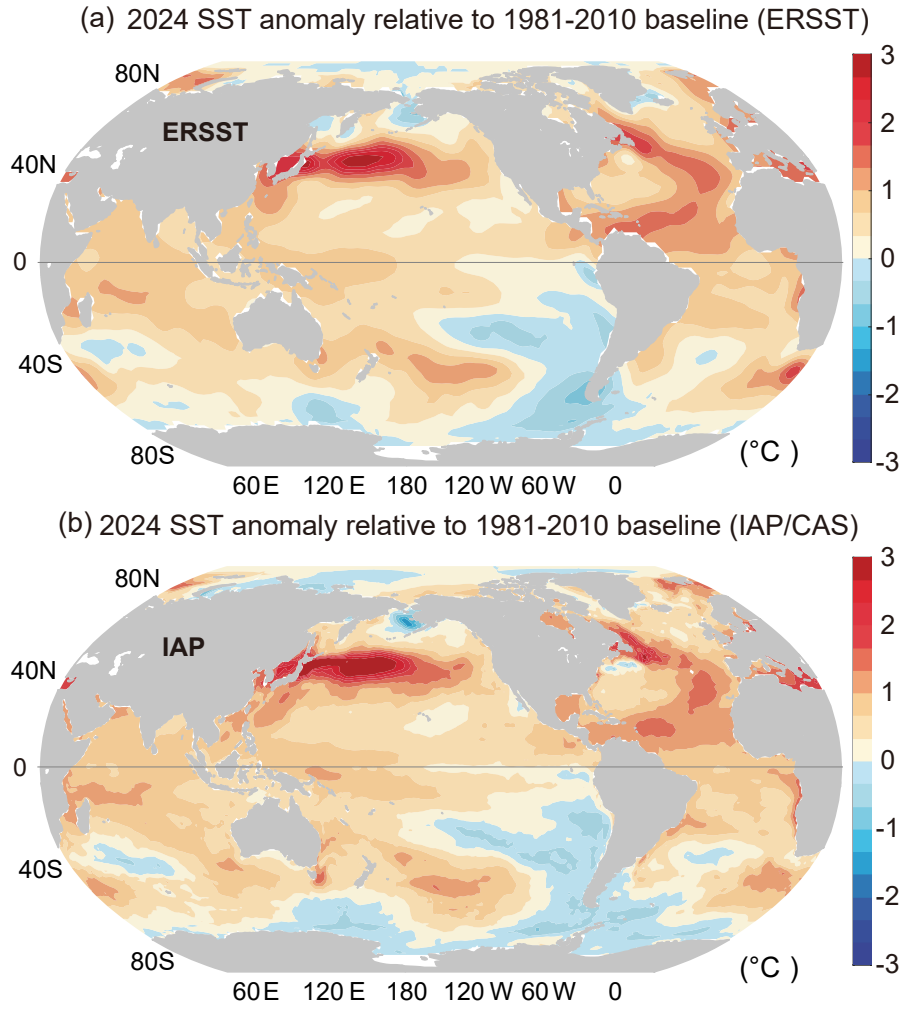

Fig. 7. The annual SST anomaly in 2024 relative to a 1981–2010 baseline for (a) ERSST and (b) IAP/CAS data separately. Units: °C.

The Southern Ocean shows a continuous long-term warming trend since the 1950s, with smaller interannual variation compared with many other regions shown in Fig. 9. The 2024–2023 OHC increase is 2.5 ZJ (0.03 GJ m^{-2}), smaller than the mean Southern Ocean warming trend in the past two decades. The recent interannual fluctuations are likely associated with ENSO (Wang et al. 2022).

There has been a striking warming trend of the North Pacific between 30°N and 65°N since the 1990s (Fig. 9), mainly in the mode and intermediate water masses of the North Pacific (Li et al. 2023), which has led to wide-ranging impacts such as an increased occurrence of marine heatwaves (Chen et al. 2023) and socioeconomic stress (Smith et al. 2021). In 2024, warming continued, with an annual OHC increase of 3.8 ZJ (0.14 GJ m^{-2}) compared to 2023, which is larger than the mean warming rate of this region over the past two decades (0.06 GJ m^{-2} yr^{-1}), mainly because the OHC in 2023 was lower than normal (Fig. 9).

The Mediterranean Sea is the region showing the most intensive warming rate, with an area-averaged OHC increase of 0.41 GJ m^{-2} (1.1 ZJ) from 2023 to 2024, higher than all the other seven regions in Fig. 9. The 2023–24 shift is around fivefold larger than the mean warming rate of this region during the past two decades and higher than the previous record shifts from 2022 to 2023 and from 1993 to 1994 of 0.32 and 0.31 GJ m^{-2}, respectively. As both global analysis and regional reanalysis datasets show very similar OHC shifts in 2024, the signal is very robust.

The tropical Atlantic and North Atlantic also continued their warming trends in 2024, with annual OHC increases of 0.03 GJ m^{-2} (0.5 ZJ) and 0.02 GJ m^{-2} (0.7 ZJ) compared to 2023, respectively (Fig. 9). The annual increases are generally consistent with the mean OHC rate over the past two decades. However, the SST in the North Atlantic was highly anomalous in 2024, and thus the ocean warming was mainly located near the sea surface—similar to 2023 conditions [see Fig. 9 in Cheng et al. (2024b)]. The 2024 Atlantic hurricane season was very active and extremely destructive.

Two other regions—the Northwest Pacific (the seas around China) and the ITF regions—show large interannual fluctuations in the OHC time series because of the dominant role of ENSO (Fig. 9). Even so, the 2024 OHC in these two regions reaches top-10 values. Both regions show decadal-scale variations as well, i.e., OHC increased from the early

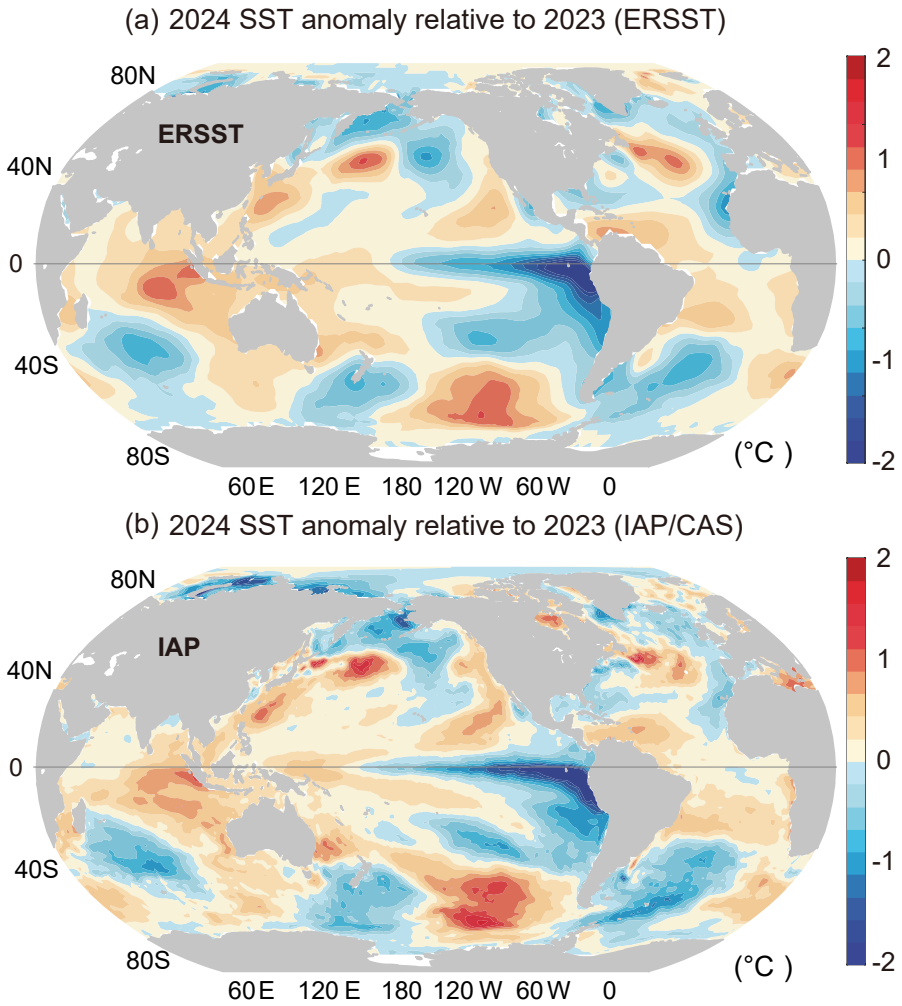

Fig. 8. (a) Differences in annual mean upper SST values between 2024 and 2023, based on (a) ERSST and (b) IAP/CAS analysis. Units: °C.

1990s to the early 2010s (Jin et al. 2024). This decadal variation has been linked to the Interdecadal Pacific Oscillation (IPO): the negative phase of the IPO leads to an OHC increase in the ITF region by driving enhanced westward ocean heat transport (Capotondi et al., 2023; Jin et al. 2024). In the Banda Sea from 1993 to 2022, there is a discernible trend of barrier layer thickness deepening by 10 m, accompanied by a reduction in mixed layer depth by 30 m, which correlates with the increase of OHC (Ismail et al., 2024).

7. Concluding remarks

Based on multiple datasets produced by several independent research groups, this paper provides updates of SST and OHC for the year 2024. We find that the ocean continued to warm globally in 2024, not only at the surface (SST) but also across the upper 2000 m (OHC). The warming rate has increased in recent decades, with a faster rate of warming evident since around 1990. Regional warming patterns reveal that six out of eight regions investigated in this study reached record levels of their upper 2000 m OHC in 2024.

The sharp increase of SST in 2023 has been heavily discussed in recent literature (e.g., Kuhlbrodt et al., 2024; Raghuraman et al., 2024; Schmidt, 2024; Goessling et al., 2025). It was partially associated with the strong El Niño event, but the post-event recovery has been modest. However, recent warming levels are not a surprise when considering the record-high OHC year after year, reflecting a positive EEI. Carbon dioxide concentrations at Mauna Loa, Hawaii, where measurements have been taken since 1958, also reached record levels in 2024 (NOAA 2024). Changes in atmospheric aerosols (visible pollution), which affect cloud coverage and brightness, are likely exacerbating warming (Gettelman et al., 2024; Wang et al., 2024; Goessling et al., 2025).

Ocean warming substantially impacts the major Earth system components. For example, ocean warming accounts for more than 1/3 of the global mean sea level rise through thermal expansion, dominating regional sea level patterns (Gulev et al., 2021). The 16 ZJ increase of OHC in 2024 compared with 2023 corresponds to a steric sea level rise of ~1.0 mm, with a total of ~54 mm since 1960. Sea level rise, in turn, increases the risk of coastal infrastructure and habitats

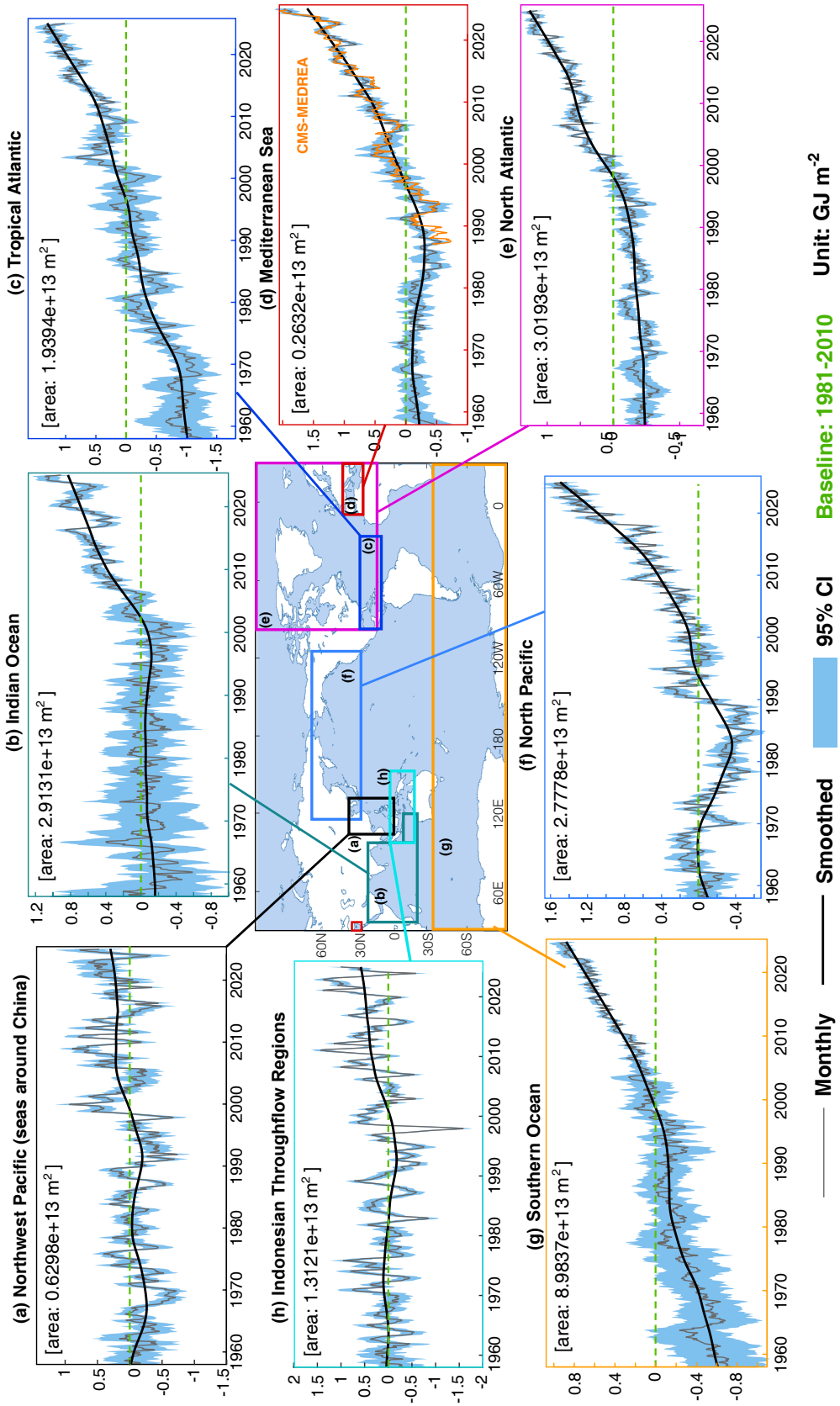

Fig. 9. Regional observed upper 2000 m OHC change from 1958 through 2024 relative to a 1981–2010 baseline using IAP/CAS data. The time series (black lines) are smoothed by LOWESS with a span width of 240 months. The gray shaded areas are the 95% confidence intervals [data updated from Cheng et al. (2024a)].

being impacted by saltwater intrusion, coastal erosion, and flooding in low-lying regions (Oppenheimer et al., 2019).

Ocean warming also exacerbates extreme weather and ocean events. These include intensification of typhoons, hurricanes, and marine heatwaves (Trenberth et al., 2018; Capotondi et al., 2024). The extra heat and moisture that enters into the atmosphere make storms more severe, with heavier rain, stronger winds, and more significant flooding (Knutson et al. 2010; Marsooli et al. 2019; Kossin et al. 2020). Warming also leads to a more rapid intensification of storms and slower decay after landfall, increasing flooding risks related to tropical cyclones (Bhatia et al. 2018, Bhatia et al. 2019; Li and Chakraborty 2020). Warming is also a factor that can cause ocean deoxygenation (Oschlies et al., 2018). Deoxygenation itself is a significant hazard for not only marine life and ecosystems, but also for humans and our terrestrial ecosystems (Bindoff et al., 2019).

According to projections based on the state-of-the-art climate models (Cheng et al. 2024a), until we reach net-zero emissions, ocean warming acceleration trend will continue (IPCC, 2021), and OHC will likely continue to break records. Better monitoring and understanding of the ocean form the basis for fostering action to assess and combat climate change, to support adaptation management, and sustainable and climate-resilient pathways (von Schuckmann et al., 2020; Abraham and Cheng, 2022; Evans et al., 2024).

Acknowledgements. The IAP/CAS analysis is supported by the National Key R&D Program of China (Grant No. 2023YFF0806500), the International Partnership Program of the Chinese Academy of Sciences (Grant No. 060GJHZ2024064MI), the Chinese Academy of Sciences and the National Research Council of Italy Scientific Cooperative Programme, the new Cornerstone Science Foundation through the XPLORER PRIZE, the National Key Scientific and Technological Infrastructure project "Earth System Science Numerical Simulator Facility" (EarthLab), and Ocean Negative Carbon Emissions (ONCE). The numerical calculations in this study were carried out by eODS (an easy-to-use Ocean observation Data processing Software package, jointly developed by CNIC and IAP) on the ORISE Supercomputer (DFZX202307). NCAR is sponsored by the US National Science Foundation. Dr. Guangcheng Li is supported by the Young Talent Support Project of Guangzhou Association for Science and Technology. We used some data collected onboard at R/V Shiyan 6, which implements the Open Research Cruise NORC2022-10+NORC2022-303 supported by NSFC shiptime Sharing Projects 42149910. The efforts of Dr. John Fasullo in this work were supported by NASA Awards 80NSSC17K0565, 80NSSC21K1191, and 80NSSC22K0046, and by the Regional and Global Model Analysis (RGMA) component of the Earth and Environmental System Modeling Program of the U.S. Department of Energy's Office of Biological & Environmental Research (BER) via National Science Foundation IA 1947282. The efforts of Dr. Alexey Mishonov were supported by NOAA (Grant No. NA19NES4320002 to CISESS-MD at the University of Maryland). The efforts of Dr. Michael Mayer were supported by the Austrian Science Fund (P33177) and ESA (contract ref. 4000145298/24/I-LR).

Data availability. The IAP/CAS data are available at http://www.ocean.iap.ac.cn/ and https://msdc.qdio.ac.cn/. The WOD is available at https://www.ncei.noaa.gov/products/world-ocean-database. The NCEI/NOAA data are available at https://www.ncei.noaa.gov/products/climate-data-records/global-ocean-heat-content. The real-time Argo data are from the China Argo Real-time Data Center (https://www.argo.org.cn/). This study has also been conducted using E.U. Copernicus Marine Service Information (https://marine.copernicus.eu/) for the Mediterranean OHC estimates. The Copernicus Marine OHC data are from https://data.marine.copernicus.eu/product/INSITU_GLO_PHY_TS_OA_NRT_013_002/description (EU Copernicus Marine Service Product, 2023a). The OSTIA data are from https://data.marine.copernicus.eu/product/SST_GLO_SST_L4_REP_OBSERVATIONS_010_011/description (EU Copernicus Marine Service Product, 2023b, c). The CO_2 data are from https://gml.noaa.gov/ccgg/trends/. GMST data from Berkeley Earth are from https://berkeleyearth.org/june-2024-temperature-update/. The Antarctic Sea Ice information is from https://nsidc.org/sea-ice-today/analyses/2024-antarctic-sea-ice-maximum-extent-finishes-second-lowest. Paris Agreement texts can be found at https://www.un.org/en/climatechange/paris-agreement. The CIGAR reanalysis is described at http://cigar.ismar.cnr.it, where there are links for data download, while the entire dataset is accessible via ftp upon request; the reanalysis uses data from the ECMWF ERA5 reanalysis (https://cds.climate.copernicus.eu/datasets/reanalysis-era5-single-levels), UKMO EN4.2.2 (https://www.metoffice.gov.uk/hadobs/en4/download-en4-2-2.html), JRA-55-do (https://climate.mri-jma.go.jp/pub/ocean/JRA55-do), COBEv2 SST (https://psl.noaa.gov/data/gridded/data.cobe2.html), and Argo data from the Coriolis/Ifremer GDAC (https://data-argo.ifremer.fr) (Argo, 2023). The NEMO model is available from https://www.nemo-ocean.eu with modifications contained in the CNR-ISMAR repository (https://baltig.cnr.it/nemo_ismar-rm/nemo_4.0.7/-/tree/3.0?ref_type=tags).

REFERENCES

Abraham, J., L. J. Cheng, M. E. Mann, K. Trenberth, and K. Von Schuckmann, 2022: The ocean response to climate change guides both adaptation and mitigation efforts. *Atmospheric and Oceanic Science Letters*, **15**, 100221, https://doi.org/10.1016/j.aosl.2022.100221.

Abraham, J. P., and L. J. Cheng, 2022: Intersection of climate change, energy, and adaptation. *Energies*, **15**, 5886, https://doi.org/10.3390/en15165886.

Argo, 2023: Argo Float Data and Metadata from Global Data Assembly Centre (Argo GDAC). SEANOE. Available from https://doi.org/10.17882/42182.

Armour, K. C., J. Marshall, J. R. Scott, A. Donohoe, and E. R. Newsom, 2016: Southern Ocean warming delayed by circumpolar upwelling and equatorward transport. *Nature Geoscience*, **9**, 549–554, https://doi.org/10.1038/ngeo2731.

Armour, K. C., and Coauthors, 2024: Sea-surface temperature pattern effects have slowed global warming and biased warming-based constraints on climate sensitivity. *Proceedings of the National Academy of Sciences of the United States of America*, **121**, e2312093121, https://doi.org/ https://doi.org/10.1073/pnas.2312093121.

Bernard, B., and Coauthors, 2006: Impact of partial steps and momentum advection schemes in a global ocean circulation model at eddy-permitting resolution. *Ocean Dynamics*, **56**, 543–567, https://doi.org/10.1007/s10236-006-0082-1.

Bhatia, K., G. Vecchi, H. Murakami, S. Underwood, and J. Kossin, 2018: Projected response of tropical cyclone intensity and intensification in a global climate model. *J. Climate*, **31**, 8281–8303, https://doi.org/10.1175/JCLI-D-17-0898.1.

Bhatia, K. T., G. A. Vecchi, T. R. Knutson, H. Murakami, J. Kossin, K. W. Dixon, and C. E. Whitlock, 2019: Recent increases in tropical cyclone intensification rates. *Nature Communications*, **10**, 635, https://doi.org/10.1038/s41467-019-08471-z.

Bindoff, N. L., and Coauthors, 2019: Changing ocean, marine ecosystems, and dependent communities. *IPCC Special Report on the Ocean and Cryosphere in a Changing Climate*, H.-O. Pörtner et al., Eds., Cambridge University Press, Cambridge, UK and New York, NY, USA, 447–587, https://doi.org/10.1017/9781009157964.007.

Boyer, T., and Coauthors, 2016: Sensitivity of global upper-ocean heat content estimates to mapping methods, XBT bias corrections, and baseline climatologies. *J. Climate*, **29**, 4817–4842, https://doi.org/10.1175/JCLI-D-15-0801.1.

Boyer, T. P., and Coauthors, 2018: World ocean database 2018. NOAA Atlas NESDIS 87.

Cai, W. J., G. Meyers, and G. Shi, 2005: Transmission of ENSO signal to the Indian Ocean. *Geophys. Res. Lett.*, **32**, L05616, https://doi.org/10.1029/2004GL021736.

Cai, W. J., and Coauthors, 2023: Southern Ocean warming and its climatic impacts. *Science Bulletin*, **68**, 946–960, https://doi.org/10.1016/j.scib.2023.03.049.

Capotondi, A., and Coauthors, 2023: Mechanisms of tropical Pacific decadal variability. *Nature Reviews Earth & Environment*, **4**, 754–769, https://doi.org/10.1038/s43017-023-00486-x.

Capotondi, A., and Coauthors, 2024: A global overview of marine heatwaves in a changing climate. *Communications Earth & Environment*, **5**, 701, https://doi.org/10.1038/s43247-024-01806-9.

Chen, H.-H., Y. T. Wang, P. Xiu, Y. Yu, W. T. Ma, and F. Chai, 2023: Combined oceanic and atmospheric forcing of the 2013/14 marine heatwave in the northeast Pacific. *npj Climate and Atmospheric Science*, **6**, 3, https://doi.org/10.1038/s41612-023-00327-0.

Cheng, L. J., J. Abraham, Z. Hausfather, and K. E. Trenberth, 2019a: How fast are the oceans warming?. *Science*, **363**, 128–129, https://doi.org/10.1126/science.aav7619.

Cheng, L. J., G. Foster, Z. Hausfather, K. E. Trenberth, and J. Abraham, 2022b: Improved quantification of the rate of ocean warming. *J. Climate*, **35**, 4827–4840, https://doi.org/10.1175/JCLI-D-21-0895.1.

Cheng, L. J., K. E. Trenberth, J. Fasullo, T. Boyer, J. Abraham, and J. Zhu, 2017a: Improved estimates of ocean heat content from 1960 to 2015. *Science Advances*, **3**, e1601545, https://doi.org/10.1126/sciadv.1601545.

Cheng, L. J., K. E. Trenberth, J. T. Fasullo, M. Mayer, M. Balmaseda, and J. Zhu, 2019b: Evolution of ocean heat content related to ENSO. *J. Climate*, **32**, 3529–3556, https://doi.org/10.1175/JCLI-D-18-0607.1.

Cheng, L. J., K. Trenberth, J. Fasullo, J. Abraham, T. Boyer, K. Von Schuckmann, and J. Zhu, 2017b: Taking the pulse of the planet. *EOS, Transactions American Geophysical Union*, **98**, 14–15, https://doi.org/10.1029/2017EO081839.

Cheng, L. J., and Coauthors, 2022a: Past and future ocean warming. *Nature Reviews Earth & Environment*, **3**, 776–794, https://doi.org/10.1038/s43017-022-00345-1.

Cheng, L. J., and Coauthors, 2024a: IAPv4 ocean temperature and ocean heat content gridded dataset. *Earth System Science Data*, **16**, 3517–3546, https://doi.org/10.5194/essd-16-3517-2024.

Cheng, L. J., and Coauthors, 2024b: New record ocean temperatures and related climate indicators in 2023. *Adv. Atmos. Sci.*, **41**, 1068–1082, https://doi.org/10.1007/s00376-024-3378-5.

Dong, Y., L. M. Polvani, and D. B. Bonan, 2023: Recent multidecadal Southern Ocean surface cooling unlikely caused by Southern Annular Mode trends. *Geophys. Res. Lett.*, **50**, e2023GL106142, https://doi.org/10.1029/2023GL106142.

Durack, P. J., and S. E. Wijffels, 2010: Fifty-year trends in global ocean salinities and their relationship to broad-scale warming. *J. Climate*, **23**, 4342–4362, https://doi.org/10.1175/2010JCLI3377.1.

Escudier, R., and Coauthors, 2020: Mediterranean Sea Physical Reanalysis (CMEMS MED-Currents, E3R1 system) (Version 1) [Data set]. Copernicus Monitoring Environment Marine Service (CMEMS), https://doi.org/10.25423/CMCC/MEDSEA_MULTIYEAR_PHY_006_004_E3R1.

Escudier, R., and Coauthors, 2021: A high resolution reanalysis for the Mediterranean Sea. *Frontiers in Earth Science*, **9**, 702285, https://doi.org/10.3389/feart.2021.702285.

EU Copernicus Marine Service Product, 2023a: Global Ocean-Real time in-situ observations objective analysis. Mercator Ocean International [data set], https://doi.org/10.48670/moi-00037.

EU Copernicus Marine Service Product, 2023b: Global Ocean OSTIA Sea Surface Temperature and Sea Ice Reprocessed. Mercator Ocean International [data set], https://doi.org/10.48670/moi-00168.

EU Copernicus Marine Service Product, 2023c: Global Ocean OSTIA Sea Surface Temperature and Sea Ice Analysis. Mercator Ocean International [data set], https://doi.org/10.48670/moi-00165.

Evans, K., and Coauthors, 2024: Delivering scientific evidence for global policy and management to ensure ocean sustainability. *Sustainability Science*, https://doi.org/10.1007/s11625-024-01579-2.

Forster, P. M., and Coauthors, 2024: Indicators of Global Climate Change 2023: Annual update of key indicators of the state of

the climate system and human influence. *Earth System Science Data*, **16**, 2625–2658, https://doi.org/10.5194/essd-16-2625-2024.

Friedlingstein, P., and Coauthors, 2023: Global carbon budget 2023. *Earth System Science Data*, **15**, 5301–5369, https://doi.org/10.5194/essd-15-5301-2023.

Gettelman, A., and Coauthors, 2024: Has reducing ship emissions brought forward global warming?. *Geophys. Res. Lett.*, **51**, e2024GL109077, https://doi.org/10.1029/2024GL109077.

Gilford, D. M., J. Giguere, and A. J. Pershing, 2024: Human-caused ocean warming has intensified recent hurricanes. *Environmental Research: Climate*, **3**, 045019, https://doi.org/10.1088/2752-5295/ad8d02.

Goessling, H. F., T. Rackow, and T. Jung, 2025: Recent global temperature surge intensified by record-low planetary albedo. *Science*, **387**, 68–73, https://doi.org/10.1126/science.adq7280.

Good, S., and Coauthors, 2020: The current configuration of the OSTIA system for operational production of foundation sea surface temperature and ice concentration analyses. *Remote Sensing*, **12**, 720, https://doi.org/10.3390/rs12040720.

Good, S. A., M. J. Martin, and N. A. Rayner, 2013: EN4: Quality controlled ocean temperature and salinity profiles and monthly objective analyses with uncertainty estimates. *J. Geophys. Res.: Oceans*, **118**, 6704–6716, https://doi.org/10.1002/2013JC009067.

Gouretski, V., L. J. Cheng, and T. Boyer, 2022: On the consistency of the bottle and CTD profile data. *J. Atmos. Oceanic Technol.*, **39**, 1869–1887, https://doi.org/10.1175/JTECH-D-22-0004.1.

Gouretski, V., F. Roquet, and L. J. Cheng, 2024: Measurement biases in ocean temperature profiles from marine mammal dataloggers. *J. Atmos. Oceanic Technol.*, **41**, 629–645, https://doi.org/10.1175/JTECH-D-23-0081.1.

Grist, J. P., and Coauthors, 2010: The roles of surface heat flux and ocean heat transport convergence in determining Atlantic Ocean temperature variability. *Ocean Dynamics*, **60**, 771–790, https://doi.org/10.1007/s10236-010-0292-4.

Gulev, S. K., and Coauthors, 2021: Changing state of the climate system. *Climate Change 2021: The Physical Science Basis. Contribution of Working Group I to the Sixth Assessment Report of the Intergovernmental Panel on Climate Change*, V. Masson-Delmotte et al., Eds., Cambridge University Press, Cambridge, United Kingdom and New York, NY, USA, 287–422, https://doi.org/10.1017/9781009157896.004.

Hansen, J., M. Sato, P. Kharecha, and K. von Schuckmann, 2011: Earth's energy imbalance and implications. *Atmospheric Chemistry and Physics*, **11**, 13 421–13 449, https://doi.org/10.5194/acp-11-13421-2011.

Hersbach, H., and Coauthors, 2020: The ERA5 global reanalysis. *Quart. J. Roy. Meteor. Soc.*, **146**, 1999–2049, https://doi.org/10.1002/qj.3803.

Hersbach, H., and Coauthors, 2023: ERA5 monthly averaged data on pressure levels from 1940 to present. Copernicus Climate Change Service (C3S) Climate Data Store (CDS), https://doi.org/10.24381/cds.6860a573.

Hu, S. J., J. Sprintall, C. Guan, M. J. McPhaden, F. Wang, D. X. Hu, and W. J. Cai, 2020: Deep-reaching acceleration of global mean ocean circulation over the past two decades. *Science Advances*, **6**, eaax7727, https://doi.org/10.1126/sciadv.aax7727.

Hu, Z. Z., M. J. McPhaden, B. Y. Huang, J. S. Zhu, and Y. Y. Liu, 2024: Accelerated warming in the North Pacific since 2013. *Nature Climate Change*, **14**, 929–931, https://doi.org/10.1038/s41558-024-02088-x.

Huang, B. Y., and Coauthors, 2017: Extended reconstructed sea surface temperature, Version 5 (ERSSTv5): Upgrades, validations, and intercomparisons. *J. Climate*, **30**, 8179–8205, https://doi.org/10.1175/JCLI-D-16-0836.1.

Huang, B. Y., and Coauthors, 2020: Uncertainty estimates for sea surface temperature and land surface air temperature in NOAAGlobalTemp version 5. *J. Climate*, **33**, 1351–1379, https://doi.org/10.1175/JCLI-D-19-0395.1.

IPCC, 2021: *Climate Change 2021: The Physical Science Basis. Contribution of Working Group I to the Sixth Assessment Report of the Intergovernmental Panel on Climate Change*. Cambridge University Press, https://doi.org/10.1017/9781009157896.

IPCC, 2023: Summary for policymakers. *Climate Change 2023: Synthesis Report. Contribution of Working Groups I, II and III to the Sixth Assessment Report of the Intergovernmental Panel on Climate Change*, Core Writing Team et al., Eds., IPCC, Geneva, Switzerland, 1–34, https://doi.org/10.59327/IPCC/AR6-9789291691647.001.

Ishii, M., A. Shouji, S. Sugimoto, and T. Matsumoto, 2005: Objective analyses of sea-surface temperature and marine meteorological variables for the 20th century using ICOADS and the Kobe Collection. *International Journal of Climatology*, **25**, 865–879, https://doi.org/10.1002/joc.1169.

Ismail, M. F. A., J. Karstensen, A. Sulaiman, B. Priyono, A. Budiman, A. Basit, A. Purwandana, and T. Arifin, 2024: Observations of barrier layer seasonal variation in the Banda Sea. *J. Geophys. Res.: Oceans*, **129**, e2023JC020829, https://doi.org/10.1029/2023JC020829.

Jin, Y. C., Y. L. Li, L. J. Cheng, J. Duan, R. Li, and F. Wang, 2024: Ocean heat content increase of the Maritime Continent since the 1990s. *Geophys. Res. Lett.*, **51**, e2023GL107526, https://doi.org/10.1029/2023GL107526.

Knutson, T. R., and Coauthors, 2010: Tropical cyclones and climate change. *Nature Geoscience*, **3**, 157–163, https://doi.org/10.1038/ngeo779.

Kossin, J. P., K. R. Knapp, T. L. Olander, and C. S. Velden, 2020: Global increase in major tropical cyclone exceedance probability over the past four decades. *Proceedings of the National Academy of Sciences of the United States of America*, **117**, 11 975–11 980, https://doi.org/10.1073/pnas.1920849117.

Kuhlbrodt, T., R. Swaminathan, P. Ceppi, and T. Wilder, 2024: A glimpse into the future: The 2023 ocean temperature and sea ice extremes in the context of longer-term climate change. *Bull. Amer. Meteor. Soc.*, **105**, E474–E485, https://doi.org/10.1175/BAMS-D-23-0209.1.

Levitus, S., and Coauthors, 2012: World ocean heat content and thermosteric sea level change (0–2000 m), 1955–2010. *Geophys. Res. Lett.*, **39**, L10603, https://doi.org/10.1029/2012GL051106.

Li, L., and P. Chakraborty, 2020: Slower decay of landfalling hurricanes in a warming world. *Nature*, **587**, 230–234, https://doi.org/10.1038/s41586-020-2867-7.

Li, Y. L., W. Q. Han, F. Wang, L. Zhang, and J. Duan, 2020: Vertical structure of the Upper-Indian Ocean thermal variability. *J. Climate*, **33**, 7233–7253, https://doi.org/10.1175/JCLI-D-19-0851.1.

Li, Z., M. H. England, and S. Groeskamp, 2023: Recent accelera-

tion in global ocean heat accumulation by mode and intermediate waters. *Nature Communications*, **14**, 6888, https://doi.org/10.1038/s41467-023-42468-z.

Loeb, N. G., G. C. Johnson, T. J. Thorsen, J. M. Lyman, F. G. Rose, and S. Kato, 2021: Satellite and ocean data reveal marked increase in Earth's heating rate. *Geophys. Res. Lett.*, **48**, e2021GL093047, https://doi.org/10.1029/2021GL093047.

Madec, G., and the NEMO System Team, 2017: *NEMO Ocean Engine*. Zenodo, https://doi.org/10.5281/zenodo.3248739.

Marsooli, R., N. Lin, K. Emanuel, and K. R. Feng, 2019: Climate change exacerbates hurricane flood hazards along US Atlantic and Gulf Coasts in spatially varying patterns. *Nature Communications*, **10**, 3785, https://doi.org/10.1038/s41467-019-11755-z.

Mayer, M., L. Haimberger, and M. A. Balmaseda, 2014: On the energy exchange between tropical ocean basins related to ENSO. *J. Climate*, **27**, 6393–6403, https://doi.org/10.1175/JCLI-D-14-00123.1.

Mayer, M., M. A. Balmaseda, and L. Haimberger, 2018: Unprecedented 2015/2016 Indo-Pacific heat transfer speeds up tropical Pacific heat recharge. *Geophys. Res. Lett.*, **45**, 3274–3284, https://doi.org/10.1002/2018GL077106.

McMonigal, K., S. Larson, S. N. Hu, and R. Kramer, 2023: Historical changes in wind-driven ocean circulation can accelerate global warming. *Geophys. Res. Lett.*, **50**, e2023GL102846, https://doi.org/10.1029/2023gl102846.

Minière, A., K. Von Schuckmann, J.-B. Sallée, and L. Vogt, 2023: Robust acceleration of Earth system heating observed over the past six decades. *Scientific Reports*, **13**, 22975, https://doi.org/10.1038/s41598-023-49353-1.

Mishonov, A., D. Seidov, and J. Reagan, 2024b: Revisiting the multidecadal variability of North Atlantic Ocean circulation and climate. *Frontiers in Marine Science*, **11**, 1345426, https://doi.org/10.3389/fmars.2024.1345426.

Mishonov, A. V., and Coauthors, 2024a: World Ocean Database 2023. NOAA Atlas NESDIS 97, https://doi.org/10.25923/z885-h264.

Nigam, T., and Coauthors, 2021: Mediterranean Sea Physical Reanalysis INTERIM (CMEMS MED-Currents, E3R1i system) (Version 1) [Data set]. Copernicus Monitoring Environment Marine Service (CMEMS), https://doi.org/10.25423/cmcc/medsea_multiyear_phy_006_004_e3r1i.

Oppenheimer, M., and Coauthors, 2019: Sea level rise and implications for low-lying islands, coasts and communities. *IPCC Special Report on the Ocean and Cryosphere in a Changing Climate*, H.-O. Pörtner et al., Eds. Cambridge University Press, Cambridge, UK and New York, NY, USA, 321–445, https://doi.org/10.1017/9781009157964.006.

Oschlies, A., P. Brandt, L. Stramma, and S. Schmidtko, 2018: Drivers and mechanisms of ocean deoxygenation. *Nature Geoscience*, **11**, 467–473, https://doi.org/10.1038/s41561-018-0152-2.

Qu, T. D, I. Fukumori, and R. A. Fine, 2019: Spin-up of the Southern Hemisphere super gyre. *J. Geophys. Res.: Oceans*, **124**, 154–170, https://doi.org/10.1029/2018jc014391.

Raghuraman, S. P., B. Soden, A. Clement, G. Vecchi, S. Menemenlis, and W. C. Yang, 2024: The 2023 global warming spike was driven by the El Niño–Southern Oscillation. *Atmospheric Chemistry and Physics*, **24**, 11 275–11 283, https://doi.org/10.5194/acp-24-11275-2024.

Rahmstorf, S., 2024: Is the Atlantic overturning circulation approaching a tipping point?. *Oceanography*, **37**(3), 16–29, https://doi.org/10.5670/oceanog.2024.501.

Ren, Q. P., Y. O. Kwon, J. Y. Yang, R. X. Huang, Y. L. Li, and F. Wang, 2024: Substantial warming of the Atlantic ocean in CMIP6 models. *J. Climate*, **37**, 3073–3091, https://doi.org/10.1175/JCLI-D-23-0418.1.

Roemmich, D., and J. Gilson, 2011: The global ocean imprint of ENSO. *Geophys. Res. Lett.*, **38**, L13606, https://doi.org/10.1029/2011GL047992.

Rohde, R. A., and Z. Hausfather, 2020: The Berkeley earth land/ocean temperature record. *Earth System Science Data*, **12**, 3469–3479, https://doi.org/10.5194/essd-12-3469-2020.

Schmidt, G., 2024: Climate models can't explain 2023's huge heat anomaly — we could be in uncharted territory. *Nature*, **627**, 467–467, https://doi.org/10.1038/d41586-024-00816-z.

Seneviratne, S. I., and Coauthors, 2021: Weather and climate extreme events in a changing climate. *Climate Change 2021: The Physical Science Basis. Contribution of Working Group I to the Sixth Assessment Report of the Intergovernmental Panel on Climate Change*, V. Masson-Delmotte et al., Eds., Cambridge University Press, Cambridge, United Kingdom and New York, NY, USA, 1513–1766, https://doi.org/10.1017/9781009157896.013.

Simpkins, G., 2024: Drivers of Southern Ocean cooling. *Nature Reviews Earth & Environment*, **5**, 4, https://doi.org/10.1038/s43017-023-00513-x.

Smith, K. E., M. T. Burrows, A. J. Hobday, A. Sen Gupta, P. J. Moore, M. Thomsen, T. Wernberg, and D. A. Smale, 2021: Socioeconomic impacts of marine heatwaves: Global issues and opportunities. *Science*, **374**, eabj3593, https://doi.org/10.1126/science.abj3593.

Smith, K. E., and Coauthors, 2023: Biological impacts of marine heatwaves. *Annual Review of Marine Science*, **15**, 119–145, https://doi.org/10.1146/annurev-marine-032122-121437.

Storto, A., 2016: Variational quality control of hydrographic profile data with non-Gaussian errors for global ocean variational data assimilation systems. *Ocean Modelling*, **104**, 226–241, https://doi.org/10.1016/j.ocemod.2016.06.011.

Storto, A., and C. X. Yang, 2024: Acceleration of the ocean warming from 1961 to 2022 unveiled by large-ensemble reanalyses. *Nature Communications*, **15**, 545, https://doi.org/10.1038/s41467-024-44749-7.

Storto, A., S. Masina, and A. Navarra, 2016: Evaluation of the CMCC eddy-permitting global ocean physical reanalysis system (C-GLORS, 1982–2012) and its assimilation components. *Quart. J. Roy. Meteor. Soc.*, **142**, 738–758, https://doi.org/10.1002/qj.2673.

Storto, A., P. Oddo, A. Cipollone, I. Mirouze, and B. Lemieux-Dudon, 2018: Extending an oceanographic variational scheme to allow for affordable hybrid and four-dimensional data assimilation. *Ocean Modelling*, **128**, 67–86, https://doi.org/10.1016/j.ocemod.2018.06.005.

Szekely, T., J. Gourrion, S. Pouliquen, and G. Reverdin, 2024: CORA, Coriolis Ocean dataset for reanalysis. SEANOE, https://doi.org/10.17882/46219.

Tan, Z. T., L. J. Cheng, V. Gouretski, B. Zhang, Y. J. Wang, F. C. Li, Z. H. Liu, and J. Zhu, 2023: A new automatic quality control system for ocean profile observations and impact on ocean warming estimate. *Deep Sea Research Part I: Oceanographic Research Papers*, **194**, 103961, https://doi.org/10.1016/j.dsr.2022.103961.

Trenberth, K. E., and Y. X. Zhang, 2019: Observed interhemi-

spheric meridional heat transports and the role of the Indonesian throughflow in the Pacific Ocean. *J. Climate*, **32**, 8523–8536, https://doi.org/10.1175/JCLI-D-19-0465.1.

Trenberth, K. E., J. T. Fasullo, and M. A. Balmaseda, 2014: Earth's energy imbalance. *J. Climate*, **27**, 3129–3144, https://doi.org/10.1175/JCLI-D-13-00294.1.

Trenberth, K. E., J. M. Caron, D. P. Stepaniak, and S. Worley, 2002: Evolution of El Niño–Southern Oscillation and global atmospheric surface temperatures. *J. Geophys. Res.: Atmos.*, **107**, AAC 5-1–AAC 5-17, https://doi.org/10.1029/2000JD000298.

Trenberth, K. E., L. J. Cheng, P. Jacobs, Y. X. Zhang, and J. Fasullo, 2018: Hurricane Harvey links to ocean heat content and climate change adaptation. *Earth's Future*, **6**, 730–744, https://doi.org/10.1029/2018EF000825.

Tsujino, H. S., and Coauthors, 2018: JRA-55 based surface dataset for driving ocean-sea-ice models (JRA55-do). *Ocean Modelling*, **130**, 79–139, https://doi.org/10.1016/j.ocemod.2018.07.002.

von Schuckmann, K., and P.-Y. Le Traon, 2011: How well can we derive Global Ocean Indicators from Argo data?. *Ocean Science*, **7**, 783–791, https://doi.org/10.5194/os-7-783-2011.

von Schuckmann, K., E. Holland, P. Haugan, and P. Thomson, 2020a: Ocean science, data, and services for the UN 2030 Sustainable Development Goals. *Marine Policy*, **121**, 104154, https://doi.org/10.1016/j.marpol.2020.104154.

von Schuckmann, K., and Coauthors, 2020b: Heat stored in the Earth system: Where does the energy go?. *Earth System Science Data*, **12**, 2013–2041, https://doi.org/10.5194/essd-12-2013-2020.

von Schuckmann, K., and Coauthors, 2024: The state of the global ocean. *8th edition of the Copernicus Ocean State Report (OSR8)*, K. von Schuckmann et al., Eds., Copernicus Publications, https://doi.org/10.5194/sp-4-osr8-1-2024.

Wang, G. J., and Coauthors, 2022: Future Southern Ocean warming linked to projected ENSO variability. *Nature Climate Change*, **12**, 649–654, https://doi.org/10.1038/s41558-022-01398-2.

Wang, H., and Coauthors, 2024: Atmosphere teleconnections from abatement of China aerosol emissions exacerbate Northeast Pacific warm blob events. *Proceedings of the National Academy of Sciences of the United States of America*, **121**, e2313797121, https://doi.org/10.1073/pnas.2313797121.

Wong, A. P. S., N. L. Bindoff, and J. A. Church, 1999: Large-scale freshening of intermediate waters in the Pacific and Indian oceans. *Nature*, **400**, 440–443, https://doi.org/10.1038/22733.

Xie, S.-P., H. Annamalai, F. A. Schott, and J. P. McCreary, 2002: Structure and mechanisms of South Indian Ocean climate variability. *J. Climate*, **15**, 864–878, https://doi.org/10.1175/1520-0442(2002)015<0864:SAMOSI>2.0.CO;2.

Yoshioka, M., D. P. Grosvenor, B. B. B. Booth, C. P. Morice, and K. S. Carslaw, 2024: Warming effects of reduced sulfur emissions from shipping. *Atmospheric Chemistry and Physics*, **24**, 13 681–13 692, https://doi.org/10.5194/acp-24-13681-2024.

Zhang, B., and Coauthors, 2024: CODC-v1: A quality-controlled and bias-corrected ocean temperature profile database from 1940–2023. *Scientific Data*, **11**, 666, https://doi.org/10.1038/s41597-024-03494-8.

Zhang, G., H. Murakami, T. R. Knutson, R. Mizuta, and K. Yoshida, 2020: Tropical cyclone motion in a changing climate. *Science Advances*, **6**, eaaz7610, https://doi.org/ https://doi.org/10.1126/sciadv.aaz7610.